

Flame Propagation in Combustion Synthesis of Ni-Ti Structural Bioimplant Material¹

LI Zhi-liang²
Olusegun J. Ilegbusi³

Abstract: This paper integrates analytical and experimental investigations of thermal and combustion phenomena during the self-propagating combustion synthesis of Ni - Ti intermetallic for structural bio-implant application. Ni - Ti mixture is prepared from elemental powders of Ni and Ti. The mixture is pressed into solid cylindrical samples of 1.1 cm diameter and 2 – 3 cm length, with initial porosity ranging from 30% to 42%. The samples are preheated to various initial temperatures and ignited from the top surface such that the flame propagates axially downwards. The flame speed images are recorded with a motion camera and the temperature profile is recorded.

Keywords: Combustion Synthesis; Intermetallic; Bio-implant material

1. INTRODUCTION

The production of certain ceramics, intermetallics, and composite materials by self-propagating high-temperature synthesis (SHS) has become increasingly popular due to its many advantages over conventional processing techniques. These benefits include low cost/energy requirements, high homogeneity of the product, reduced microstructural segregation, low contamination, and the relative simplicity of the process (YI & Moore, 1990; LU & Hirohashi, 1999; Yeh & Yeh, 2005; Zanotti et al., 2007; Biswas, 2005). The growing popularity of SHS has led to a number of experimental, theoretical and numerical studies aimed at improving fundamental understanding of the process (YI & Moore, 1990; LU & Hirohashi, 1999; Yeh & Yeh, 2005; Zanotti et al., 2007; Biswas, 2005; LI et al., 2000; Margolis, 1992). However, existing theoretical and numerical studies have typically relied on oversimplifications such as the assumption of constant thermal conductivity throughout the specimen. Further work is therefore desirable to elucidate the effects of process parameters and variable thermophysical properties on the synthesis. This is the primary objective of the present paper.

¹ This work was supported by the US National Science Foundation under contract number NSF-CMMI-0854208.

² Dept. of Mechanical, Materials and Aerospace Engineering, University of Central Florida, Orlando, FL 32816-2450, USA.

³ Dept. of Mechanical, Materials and Aerospace Engineering, University of Central Florida, Orlando, FL 32816-2450, USA. Email: ilegbusi@mail.ucf.edu.

*Received 16 May 2010; accepted 8 July 2010

By definition, SHS involves initiating an exothermic, condensed-phase chemical reaction between two or more species to obtain the desired product. Although under the appropriate conditions the exothermic nature of the reaction allows the process to become steadily self-sustaining, SHS is very sensitive to the process parameters and material properties, and other reaction patterns are possible (i.e. oscillatory propagation, fingering, and reaction extinction) (ZHANG & Stangle, 1994; Puszynski et al., 1985; RAO et al., 1994; Bertolino et al., 2003).

In order to fully realize the potential of SHS, it is imperative that the individual and cumulative effects of the various material and process parameters on the characteristics of both the reaction and the final product be fully understood. Process parameters such as preheat temperature, porosity, and the amount of reactant dilution, have all been shown experimentally to have a strong effect on the behavior of the combustion synthesis process (Yeh & Yeh, 2005; Zanotti et al., 2007; Puszynski et al., 1985; YI & Moore, 1989; YI & Moore, 1989; Advani et al., 1992; Bhattacharya, 1992; Bhattacharya, 1991; Lakshmikantha et al., 1992). The material properties of the various phases also influence the reaction significantly (Margolis, 1992; Puszynski et al., 1985; Lakshmikantha et al., 1992; Puszynski et al., 1987). Thus, there have been numerous attempts to model SHS to study the process through numerical experiments and to apply existing knowledge for optimization of industrial SHS processes. Experimental data and numerical analysis both suggest that the effective thermal conductivity, k_{eff} , is one of the most important parameters impacting reaction behavior during combustion synthesis (Yeh & Yeh, 2005; ZHANG & Stangle, 1994; Advani et al., 1992; Matson & Munir, 1992; ZHANG & Stangle, 1994).

In the present study, an experimental apparatus is set up to investigate Ni - Ti intermetallic processing using combustion synthesis. It focuses at this stage on the effect of processing conditions on the flame front propagation speed. Compressed Ni - Ti powder cylindrical samples for are used to investigate the flame speed and effective thermal conductivity over a range of initial sample porosities. Specifically, the difference in the effective thermal conductivity on either side of the reaction front is investigated..

2. PROBLEM CONSIDERED

Figure 1 illustrates the combustion synthesis process and the associated differences in effective thermal conductivity for the reactant, combustion and product phases. Although in practice these differences in thermal conductivity may be either material or process dependent, the exact source is of less concern than the overall effect on the propagation of the reaction front (Ballas et al., 2006). The source will thus not be specifically addressed in this paper.

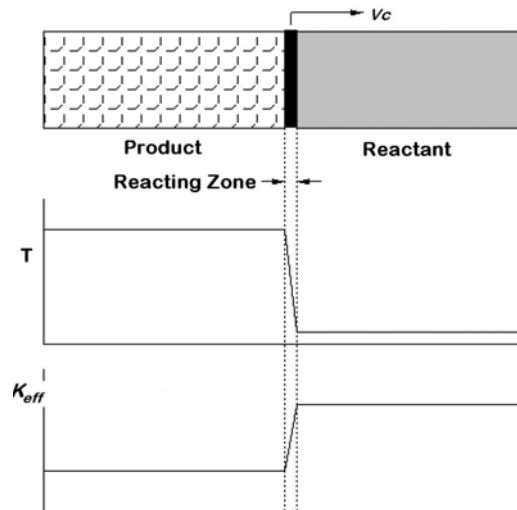


Fig. 1: Schematic of the combustion synthesis process, the corresponding temperature profile, and the effective thermal conductivity for the reactant, combustion and product regions

3. EXPERIMENTAL APPARATUS AND PROCEDURE

Figure 2 shows the experimental apparatus used for the study. It consists of a stainless steel iso-velocity Argon flow controller, an insulator, a heating wire, an ignition wire, a motion camera and an infrared sensor. Cylindrical samples of Ni – Ti intermetallic were prepared from elemental powders of Ni (99.9% purity, 100 mesh, particle size ≤ 0.149 mm) and Ti (99.5% purity, 100 mesh, particle size ≤ 0.149 mm), homogeneously dry-mixed in the stoichiometric ratio 1:1 in Argon flow purging environment. The powders were cold pressed into cylindrical samples (1.11 cm diameter) with the CARVER manual hydraulic press. The press exerts force on the top surface of the sample, ranging from 3000 lb to 7000 lb. The corresponding porosities of the samples ranged from 42% to 30%. All the tests were carried out in a stainless steel iso-velocity Argon flow controller in an open air environment and monitored with a Redlake Motion camera and an infrared temperature sensor. Each Ni - Ti sample was set on top of an insulator within a solenoid Nichrome heating coil. The heating was controlled by a DC power supply (HY3030E) with the capability to uniformly preheat the sample to any prescribed temperature up to 700°C within 10 minutes.

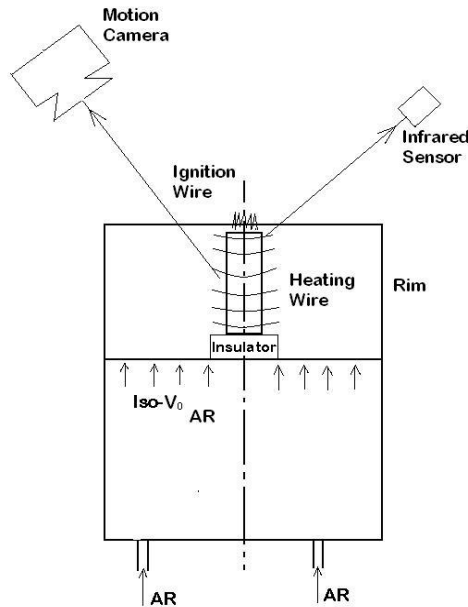


Fig. 2: Schematic of experimental apparatus

A zigzag tungsten ignition wire (0.5 mm diameter) was set up approximately 2 mm above the top surface of the sample. The ignition current was controlled by another DC power supply (HY3050E). The ignition energy was delivered by radiation heat transfer through the 2 mm gap between the ignition wire and sample surface. The preheating and combustion temperature were acquired using infrared sensor (MICRO EPSILON, thermometer CTM-2). The temperature data were gathered by the data acquisition system at an interval of 10 ms via USB interface. In addition, in order to verify the accuracy of the infrared sensor and adjust the material emissivity coefficient, a thermocouple (OMEGA, K type, bead size 0.12 mm and response time of about 10 ms) was used to probe the sample surface several times before the ignition. The combustion front propagation speed was then determined from the images of the reaction front position, which was recorded by the motion camera system at a frequency of 50 f/sec.

4. CFD-AIDED DESIGN OF ARGON PURGE FLOW CONTROL

The top surface of the experimental apparatus was designed to be exposed to air ambience for convenient observation of temperature and flame speed data as well as ease the preheating and ignition power cable connection. Thus argon flow was needed to purge oxygen from the Ni - Ti sample surface. A certain

average flow velocity (V_0) would be required to ensure that the oxygen fraction on the sample surface was negligible while also ensuring that the argon usage and heat loss were small.

A Computational Fluid Dynamics (CFD) model was therefore used to predict this argon flow velocity for design of the experiment. For a typical experimental process, the preheating time usually endures for 10 minutes, the ignition process lasts for 10 - 60 seconds, and the flame front propagates from the top to the bottom in about 3 seconds. Thus, our main concern of inadvertent oxidization was in the preheating phase. For simplification, the following two representative steady state simulations were considered in the preheating phase:

(a) Low preheating temperature simulation

Boundary conditions:

Heating wire = 630 °C; Ni - Ti Cylinder surface = 330 °C; Insulator surface = 130 °C.

(b) High preheating temperature simulation

Boundary conditions:

Heating wire = 930 °C; Ni - Ti Cylinder surface = 550 °C; Insulator surface = 230 °C.

The preliminary calculations done using CFD are presented in Figs 3 and 4 for low and high preheating temperatures respectively. Specifically, each figure presents the predicted distribution of oxygen mole fraction as a function of axial and radial position, x and r respectively, around the sample. The predictions show that for both low and high preheating temperature simulations, the maximum mole fractions of oxygen on the Ni - Ti sample will fall below 0.01% for the average argon flow velocity $V_0 = 3$ cm/s. This value is thus considered sufficient argon purge flow velocity to ensure negligible oxygen environment and used for design of the experiment.

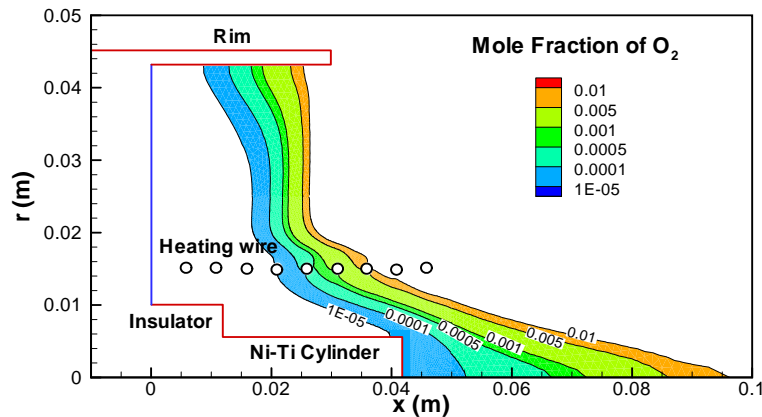


Fig. 3: Contours of mole fraction of oxygen for $V_0 = 3$ cm/s in low preheating state

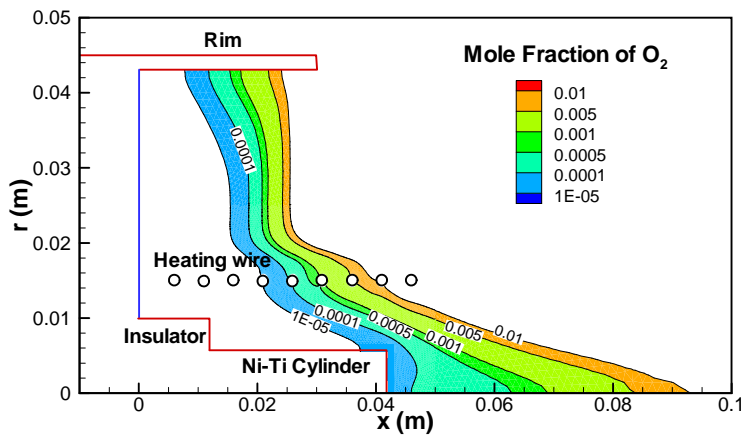


Fig. 4: Contours of mole fraction of oxygen for $V_0 = 3$ cm/s in high preheating state

5. RESULT AND DISCUSSION

The combustion synthesis of Ni-Ti intermetallic material is largely determined by the processing parameters, including the sample porosity, particle size, and preheat temperature. The samples have to be preheated above a specific temperature to be ignited by the tungsten ignition wire above the top surface. This implies the reactions between Ni and Ti are not sufficiently exothermic for self-sustainable flame propagation. Figure 5 shows a typical SHS process recorded by the motion camera at different instances, using the cylindrical sample of 35% initial porosity and preheated to 550 °C. After ignition a bright and self-sustained flame front propagates downward as a nearly parallel (one-dimensional similarity) flame front from the ignited top surface and transfers the preheated reactant into an incandescent combustion product. The flame front propagation velocity was found to be approximately constant, based on the flame front trajectory extracted from the motion camera frames, which was set up to take 50 frames per second at an exposure of 1/200 second. It took approximately 2 seconds for the flame front to travel from the top of the sample to the bottom over a length of 2.8 cm. The sample continued to glow and melt down even after 2.8 seconds. After 5 seconds, the luminosity on the sample gradually faded away due to the heat loss to the environment. This phenomenon indicates that the flame propagation speed was much higher than the reaction rate, thus the reaction zone was not restricted to the flame front, but continued vigorously in the bulk behind the flame front.

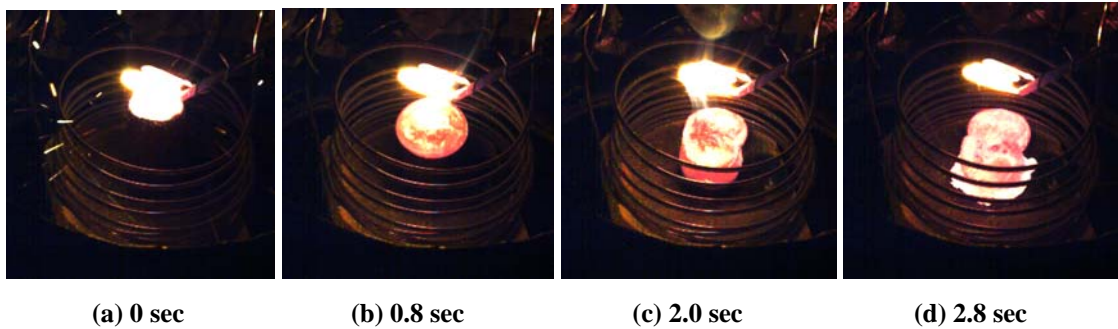


Fig. 5: Recorded combustion for 35% initial porosity, 100 mesh Ni - Ti particles ignited with 550 °C preheating.

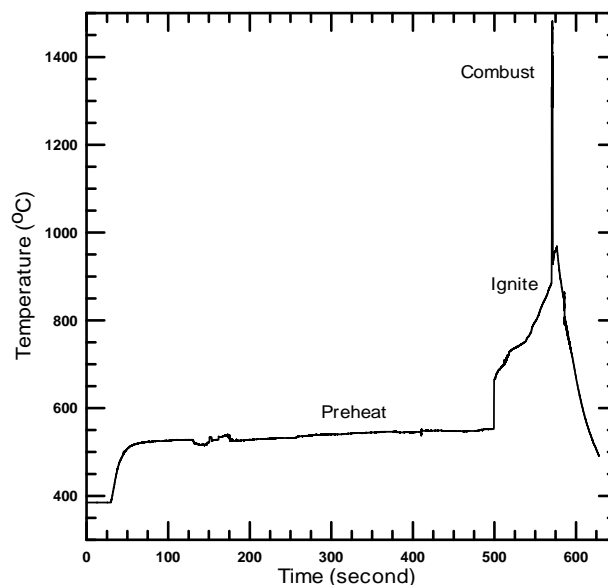


Fig. 6: Temperature v.s. Time graph of sample surface for SHS 35% initial porosity, 100 mesh Ni - Ti particles ignited with 550 °C preheating.

An infrared temperature sensor was applied to record the temperature data and the emissivity for Ni-Ti sample surface was set to 0.55. This value was verified by the thermocouple measurement when the sample surface was heated to 700 °C. However, the emissivity data varies with the surface temperature, especially when the sample starts to burn and melt, so the error in the recorded temperature for the combusted high temperature surface is relatively high (20 °C). Figure 6 shows the temperature versus time graph at one point (diameter 1.8 mm) on the top of the cylinder side face for the SHS process utilizing a sample with 35% initial porosity, 100 mesh Ni - Ti particles ignited with 550 °C preheating. The sample was slowly preheated to 550 °C, and then the ignition power was abruptly turned on. The sample top surface was subsequently heated to 900 °C within 60 seconds.

Figure 7 is an amplified version of the previous Fig. 6 with focus on the time duration about 670s to 671s. This figure shows the temperature distribution in the system as the flame propagates through that layer. The temperature increases from 920 °C (ignition temperature for Ni - Ti particle mixture (Zanotti et al., 2007; Bertolino et al., 2003)) to 1310 °C within 0.1 second, remains flat around 1310 °C for a short period and increases to 1460 °C after 0.8 second. This is because the Ni - Ti alloy absorbed the latent heat from the exothermic reactions at the melting point (1310 °C). After approximately 0.8 second, the exothermic reactions terminate, and the bulk begins to cool down due to heat loss. Meanwhile the flame front has propagated over a distance of $2.8 \text{ cm} \times 0.8 \text{ sec} / 2.0 \text{ sec} = 1.12 \text{ cm}$, which is the solid flame thickness. However, the temperature increase is concentrated in the flame front layer with thickness $2.8 \text{ cm} \times 0.06 \text{ sec} / 2.0 \text{ sec} = 0.84 \text{ mm}$, and a temperature gradient of $(1270 \text{ °C} - 920 \text{ °C}) / 0.84 \text{ mm} = 417 \text{ °C/mm}$. As the flame front propagates downward, the temperature difference on the flame front will be even larger because this zone is not heated by the tungsten ignition wire. The region remains approximately at the preheat temperature of 550 °C before the flame front approaches and initiates the reactions. Therefore, the thermal conductivity and heat transfer in the preheated layer (i.e the zone from 550°C to 920°C) and flame front layer (920 °C to 1270 °C) are critical to the flame front propagation velocity. The thermal conductivity and heat transfer in the flat temperature region comprising the melted Ti - Ni alloy is not important.

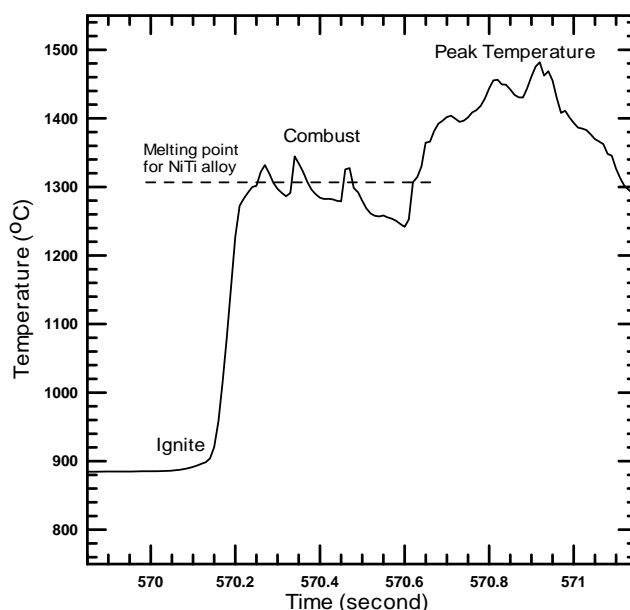


Fig. 7: Amplified Temperature v.s. Time graph of the sample surface for 35% initial porosity, 100 mesh Ni - Ti particles ignited with 550 °C preheating.

The higher preheat temperature indicates a smaller temperature barrier between the green reactant and the ignition point. Thus, for the same thermal conductivity properties the flame front propagation velocity will be significantly increased. Figure 8 shows the dependence of the flame front velocities and product temperatures on preheat temperatures associated with 35% initial porosity. The flame front velocities monotonously increase from 9.8 mm/s to 16.2 mm/s, when the preheat temperature increases from 480 °C to 580 °C. The measured product maximum surface temperature which has an error of $\pm 20 \text{ °C}$ for the liquid alloy surface ($>1310 \text{ °C}$) also agrees satisfactorily with the preheat temperature.

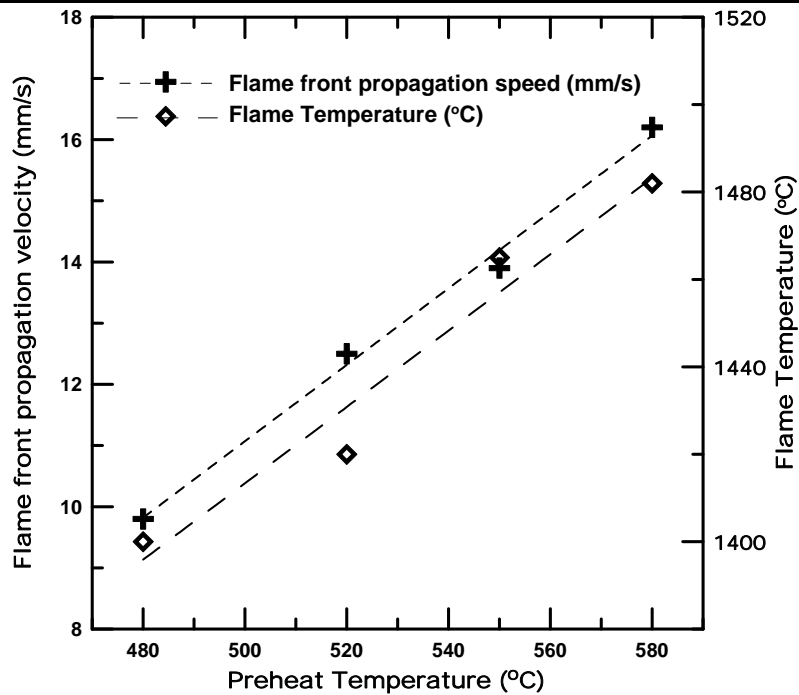


Fig. 8: Dependence of combustion front velocity and product temperature on preheat temperature for the 35% initial porosity, 100 mesh particle size.

The effective thermal conductivity k_{eff} is solely determined by the initial porosity for the specified particle ratio and size. Figure 9 indicates that the flame front velocities continuously increase with reduced initial sample porosity. On the other hand, k_{eff} monotonously increases with the reduction of the initial sample porosity.

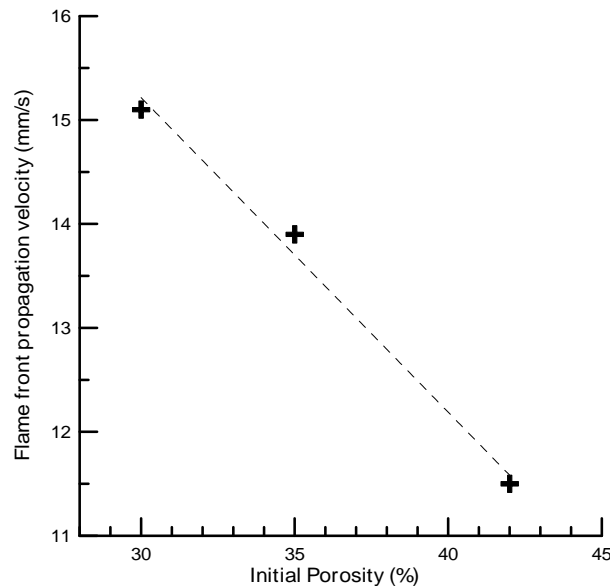


Fig. 9: Dependence of combustion front velocity on initial cylinder sample porosity with 550 °C preheating.

REFERENCES

A. Biswas. (2005). *Acta Mater* 53: 1415.

- A.H. Advani, N.N. Thadhani, H.A. Grebe, R. Heaps, C. Coffin, and T. Kottke. (1992). "Dynamic modelling of material and process parameter effects on self-propagating high-temperature synthesis of titanium carbide ceramics." *Journal of Materials Science*, 27: 3309--3317.
- A.K. Bhattacharya. (1992). "Modelling of the effects of porosity and particle size on the steady-state wave velocity in combustion synthesis." *Journal of Materials Science*, 27(6): 1521--1527.
- A.K. Bhattacharya. (1991). "Green density of a powder compact and its influence on the steady-state wave velocity in combustion synthesis of condensed phase." *Journal of the American Ceramic Society*, 74(9): 2113--2116.
- C. L. Yeh and C.C. Yeh. (2005). "Preparation of CoAl intermetallic compound by combustion synthesis in self-propagating mode". *Journal of Alloys and Compounds*, 288:241-249.
- C. Zanotti, P. Giuliani, A. Terrosu, S. Gennari and F. Maglia. (2007). "Porous Ni-Ti ignition and combustion synthesis." *Intermetallics*, 15:404-412,.
- D.M. Matson and Z.A. Munir. (1992). "Combustion synthesis of intermetallic compounds using titanium nickel and copper wires." *Materials Science and Engineering*, 153A(1/2): 700—705.
- J. Puszynski, J. Degreve, and V. Hlavacek. (1987). "Modeling of exothermic solid-solid noncatalytic reactions." *Industrial and Engineering Chemistry Research*, 26(7): 1424--1434.
- J. Puszynski, V.K. Jayaraman, and V. Hlavacek. (1985). "A Stefan problem for exothermic non-catalytic reactions." *International Journal of Heat and Mass Transfer*, 28(6): 1237--1239.
- LI B.-Y., L.-J. Rong, LI Y.-Y., and V.E. Gjunter. (2000). "Fabrication of cellular NiTi Intermetallic compounds." *Journal of Materials Research*, 15(1):10-13.
- LU Y and M.~Hirohashi. (1999). "Thermal behavior during combustion synthesis of intermetallic compound of Ni--Al system." *Journal of Materials Science Letters*, 18(5): 395--398.
- M. Ballas, SONG H. and O. J. Ilegbusi. (2006). "Effect of thermal conductivity on reaction front propagation during combustion synthesis of intermetallics." *Journal of material science*, 41: 4169-4177.
- M.G. Lakshmikantha, A. Bhattacharya, and J.A. Sekhar. (1992). "Numerical modeling of solidification combustion synthesis." *Metallurgical Transactions*, 23A(1): 23--34.
- N. Bertolino, M. Monagheddu, A. Tacca, P. Giuliani, C. Zanotti and U. A. Tamburini. (2003). "Ignition mechanism in combustion synthesis of Ti-Al and Ti-Ni systems." *Intermetallics*, 11: 41.
- RAO L., YU P., and R.B. Kaner. (1994). "Numerical modeling of combustion synthesis with phase changes." *Journal of Materials Synthesis and Processing*, 2(6): 343--353.
- S.B. Margolis. (1992). "The asymptotic theory of gasless combustion." *Metallurgical Transactions*, 23A(1): 15--22.
- YI H.C. and J.J. Moore. (1989). "Combustion synthesis of of TiNi intermetallic compounds. Part 1, Determination of heat of fusion of TiNi and heat capacity of liquid TiNi." *Journal of Materials Science*, 24(10): 3449--3455.
- YI H.C. and J.J. Moore. (1989). "Combustion synthesis of of TiNi intermetallic compounds. Part 2. Effect of TiO₂ formation." *Journal of Materials Science*, 24(10): 3456--3462.
- YI H.C and J.J. Moore. (1990). "The combustion synthesis of Ni--Ti shape memory alloys." *The Journal of the Minerals, Metals, and Materials Society*, 42(8): 31--35.
- Y. Zhang and G.C. Stangle. (1994). "A micromechanistic model of the combustion synthesis process: Part I. Theoretical development." *Journal of Materials Research*, 9(10): 2592--2604.

ZHANG Y. and G.C. Stangle. (1994). "A micromechanistic model of the combustion synthesis process: Part II. Numerical simulation." *Journal of Materials Research*, 9(10): 2605--2619.

LIST OF FIGURES

Fig. 1: Schematic of the combustion synthesis process, the corresponding temperature profile, and the effective thermal conductivity for the reactant, combustion and product regions. Fig. 2: Schematic of experimental apparatus.

Fig. 3: Contours of mole fraction of oxygen for $V_0 = 3$ cm/s in low preheating state

Fig. 4: Contours of mole fraction of oxygen for $V_0 = 3$ cm/s in high preheating state

Fig. 5: Recorded combustion for 35% initial porosity, 100 mesh Ni - Ti particles ignited with 550 oC preheating.

Fig. 6: Temperature v.s. Time graph of sample surface for SHS 35% initial porosity, 100 mesh Ni - Ti particles ignited with 550 oC preheating.

Fig. 7: Amplified Temperature v.s. Time graph of the sample surface for 35% initial porosity, 100 mesh Ni-Ti particles ignited with 550 oC preheating.

Fig. 8: Dependence of combustion front velocity and product temperature on preheat temperature for the 35% initial porosity, 100 mesh particle size.

Fig. 9: Dependence of combustion front velocity on initial cylinder sample porosity with 550 oC preheating.